pISSN 2384-1095
eISSN 2384-1109

iMRI 2017;21:20-27

https://doi.org/10.13104/imri.2017.21.1.20

iMRI
Investigative Magnetic Resonance Imaging

Assessment of Left Ventricular Function with Single Breath-Hold Magnetic Resonance Cine Imaging in Patients with Arrhythmia

So Hyeon Bak[1,2], Sung Mok Kim[1,3], Sung-Ji Park[3,4], Min-Ji Kim[5], Yeon Hyeon Choe[1,3]

[1]Department of Radiology, Samsung Medical Center, Sungkyunkwan University School of Medicine, Seoul, Korea
[2]Department of Radiology, Kangwon National University Hospital, Chuncheon, Korea
[3]Cardiovascular Imaging Center, Heart Vascular Stroke Institute, Samsung Medical Center, Sungkyunkwan University School of Medicine, Seoul, Korea
[4]Department of Cardiology, Department of Medicine, Samsung Medical Center, Sungkyunkwan University School of Medicine, Seoul, Korea
[5]Biostatistics and Clinical Epidemiology Center, Samsung Medical Center, Seoul, Korea

Original Article

Received: January 5, 2017
Revised: March 16, 2017
Accepted: March 16, 2017

Correspondence to:
Sung Mok Kim, M.D., Ph.D.
Department of Radiology and Cardiovascular Imaging Center, Heart Vascular Stroke Institute, Samsung Medical Center, Sungkyunkwan University School of Medicine, 81 Ilwon-ro, Gangnam-gu, Seoul 06351, Korea.
Tel. +82-2-3410-2519
Fax. +82-2-3410-2559
E-mail: sungmok_kim@hanmail.net

Purpose: To evaluate quantification results of single breath-hold (SBH) magnetic resonance (MR) cine imaging compared to results of conventional multiple breath-hold (MBH) technique for left ventricular (LV) function in patients with cardiac arrhythmia.

Materials and Methods: MR images of patients with arrhythmia who underwent MBH and SBH cine imaging at the same time on a 1.5T MR scanner were retrospectively reviewed. Both SBH and MBH cine imaging were performed with balanced steady state free precession. SBH scans were acquired using temporal parallel acquisition technique (TPAT). Fifty patients (65.4 ± 12.3 years, 72% men) were included. End-diastolic volume (EDV), end-systolic volume (ESV), stroke volume (SV), ejection fraction (EF), myocardial mass, and LV regional wall motion were evaluated.

Results: EF, myocardial mass, and regional wall motion were not significantly different between SBH and MBH acquisition techniques (all P-values > 0.05). EDV, ESV, and SV were significant difference between the two techniques. These parameters for SBH cine imaging with TPAT tended to lower than those in MBH. EF and myocardial mass of SBH cine imaging with TPAT showed good correlation with values of MBH cine imaging in Passing-Bablok regression charts and Bland-Altman plots. However, SBH imaging required significantly shorter acquisition time than MBH cine imaging (15 ± 7 sec vs. 293 ± 104 sec, P < 0.001).

Conclusion: SBH cine imaging with TPAT permits shorter acquisition time with assessment results of global and regional LV function comparable to those with MBH cine imaging in patients with arrhythmia.

Keywords: Temporal parallel acquisition technique; Single breath-hold cine magnetic resonance; TGRAPPA; Arrhythmia; Left ventricular function

INTRODUCTION

Accurate and reproducible assessment of global left ventricular (LV) function is essential for clinical diagnosis, risk identification, estimation of prognosis, and treatment of cardiovascular disease (1, 2). Electrocardiogram (ECG)-gated multiple breath-hold (MBH) cine magnetic resonance imaging (MRI) has been regarded as the standard of reference for precise evaluation of LV function due to its high signal-to-noise ratio (SNR), high contrast-to-noise ratio (CNR), and excellent temporal resolution (3, 4). The precise quantitative evaluation of LV function with MBH cine MRI is based on a parallel stack of short-axis slices with steady-state free precession (SSFP) cine pulse sequence from LV base to apex. Each slice is obtained during breath-hold. SSFP yields excellent endocardial contour contrast. It facilitates accurate and automated segmentation of endocardial and epicardial contours to analyze ventricular function (1, 5).

However, ECG-gated MBH cine MRI using SSFP technique is time consuming for LV function with whole-ventricle acquisition time up to 12 min (6-8). Additionally, heart rate and rhythm of patients must be regular to obtain adequate images. Blurring of cine images may occur in patients with arrhythmia (9). Therefore, evaluation of LV function in patients with arrhythmia is limited as data acquisition is synchronized to cardiac rhythm and spread over multiple heart beats.

Temporal parallel acquisition technique (TPAT) permits more rapid image acquisition as this technique skips phase encoding steps and reconstructs missing k-space lines from multi-element coil sensitivity profiles (10). However, TPAT can result in reduced SNR but increased artifact (9). A previous study has reported the feasibility of using accelerated cine MRI for tachycardia (11). However, their data were obtained from an animal study. Therefore, the objective of the present study was to assess quantification results of single breath-hold (SBH) MR cine imaging compared to results from conventional MBH technique for LV function in patients with cardiac arrhythmia.

MATERIALS AND METHODS

Study Population

This retrospective study was approved by our Institutional Review Board. Informed consent was waived due to its retrospective nature. Between February 2012 and April 2015, 50 consecutive patients with arrhythmia who underwent both MBH and SBH cine MRI at the same time were enrolled. Patients enrolled in the study had several classes of arrhythmias, including atrial fibrillation (n = 15), atrial flutter (n = 2), ventricular tachycardia (n = 2), ventricular premature contraction (n = 10), atrial premature contraction (n = 4), atrioventricular block (n = 6), left anterior fascicular block (n = 2), sinus bradycardia/tachycardia (n = 6), paroxysmal supra-ventricular tachycardia (n = 2), and right bundle branch block (n = 1). All patients were clinically indicated for cardiovascular magnetic resonance (CMR) imaging based on various pathologies: myocardial infarction, n = 15; cardiomyopathy, n = 19; valvular heart disease, n = 10; heart failure, n = 2; pericardial disease, n = 2; amyloidosis, n = 1; and pulmonary artery hypertension, n = 1.

Cardiovascular Magnetic Resonance (CMR)

CMR images were obtained using a 1.5-T MR system (Magnetom Avanto; Syngo MR B17 version; Siemens Medical Solution, Erlangen, Germany) equipped with a maximum strength gradient of 45 mT/m, a slew rate of 200 mT/m/msec, and a 32-channel body array coil. CMR scans consisted of localizing images (axial, coronal, and sagittal) and cine scans (2-chamber view, 3-chamber view, 4-chamber view, and short-axis view). All scans were carried out by qualified technicians and supervised by an experienced radiologist.

After acquisition of scout images, balanced SSFP cine images with generalized auto-calibration of partially parallel acquisitions (GRAPPA; Siemens Medical Solutions, Erlangen, Germany) reconstruction algorithm were obtained during MBH. LV short-axis images were acquired at 10 mm intervals (6 mm thickness with intersection gap of 4 mm) from LV base to apex in order to include the entire LV volume by using retrospective ECG-gating with the following parameters: repetition time/echo time, 3.13 msec/1.31 msec; flip angle, 72°; field of view, 240 × 300 mm^2; matrix, 256 × 150; spatial resolution, 1.29 × 1.29 mm; temporal resolution, 50.08 ms; and GRAPPA acceleration factor, 2. Within one R-R interval, 30 contiguous images were acquired for each slice level.

SBH cine imaging over the whole LV volume was performed in short-axis slices using a combined GRAPPA-accelerated SSFP sequence and a TPAT reference scanning mode with prospective ECG-gating. The following parameters were used: repetition time/echo time, 2.68 msec/1.16 msec; flip angle, 72°; field of view, 240 × 300

mm^2; and matrix, 256 × 150; spatial resolution, 1.98 × 1.98 mm; temporal resolution, 80.40 ms; and acceleration factor, 3. SBH images were acquired directly after MBH images. Within one R-R interval, 6 to 14 contiguous images were acquired depending on heart rate.

Cardiovascular Magnetic Resonance Analysis

CMR image analyses were performed by two independent investigators (S.H.B. and S.M.K. with 6 and 10 years of experience, respectively) who were blinded to clinical results and each other's assessment. Each reader analyzed either SBH cine imaging with TPAT or the standard single-slice imaging.

Quantitative evaluation of LV volume and mass was performed for the end of diastole and the end of systole. Frames with the largest and smallest ventricular volumes were chosen as end diastole and end systole, respectively. LV end-diastolic volume (LVEDV), LV end-systolic volume (LVESV), LV ejection fraction (LVEF), and LV mass were calculated from short-axis cine images using ARGUS™ software (Siemens Healthcare, Erlangen, Germany). Manual editing of automatically segmented endocardial and epicardial borders was performed for all data-sets. Papillary muscles and endocardial trabeculations were included in the calculation of LV volume. LV mass was measured by multiplying the sum of total LV myocardial volumes from cine images by specific gravity of the myocardium.

Qualitative analysis of regional wall motion was performed on short-axis cine images. Regional wall motion abnormalities were classified as normal, hypokinesia, or akinesia for 16 segments based on the standard American Heart Association's (AHA) segmentation except for apex (12). Regional wall motion abnormalities were graded for each segment using the following classification system: 1 = normal, 2 = hypokinesia, and 3 = akinesia (13). Regional wall motion analysis was performed for 800 segments in each technique. A total of 1600 segments were analyzed. Difference in measured values by both investigators were resolved by their final consensus. Consensus values were used to analyze LV function and regional wall motion.

SNR and CNR were calculated using region of interest (ROI) for signal and noise. For SNR and CNR evaluation, mean signal intensity within septum and lateral wall of left ventricle, signal intensity of LV cavity, an mean standard deviation (SD) of background noise in two different ROI were assessed at mid-ventricular level on short-axis view. The mean value measured by the two investigators was used for the analysis. SNR was calculated as the signal intensity of the myocardium divided by the SD of background noise. CNR was measured as the difference between the signal intensity of LV cavity and that of the myocardium divided by the SD of background noise. Regions with obvious artifact were avoided for the evaluation of SNR and CNR.

Statistical Analysis

Continuous variables were expressed as mean ± SD. Bland-Altman plot and Passing-Bablok regression charts were employed to examine the degree to which the two techniques produced the same results of volumetric data. LV functional parameters and myocardial mass were compared between the two techniques using paired t-test or Wilcoxon signed rank test. Difference in observed numbers of segments with wall motion abnormality between the two techniques was compared using McNemar's test. Inter-observer agreement for measurement of LV functional parameters and regional wall motion was assessed using intra-class correlation coefficient (ICC) and weighted kappa analysis. Wilcoxon signed rank test was used to assess any difference between SNR and CNR of the two techniques. For all data analyses, a P-value of less than 0.05 was considered statistically significant. All analyses were performed using SAS version 9.4 (SAS Institute, Cary, NC, USA) and R 3.2.5 (Vienna, Austria; http://www.R-project.org/).

RESULTS

Fifty patients with arrhythmia (36 men, 14 women; mean age, 65.4 ± 12.3 years; range, 38 to 89 years) were included in this study. Semiautomatic contour drawing was feasible in all patients for MBH and SBH cine images. SBH cine imaging with TPAT required substantially shorter acquisition time than MBH cine imaging (15.7 ± 7 sec vs. 293 ± 104 sec, $P < 0.001$). The image number of contiguous cine images was 30 in MBH and 10.3 ± 2.8 in SBH technique.

Results of volumetric analysis and myocardial mass of MBH and SBH cine imaging are summarized in Table 1. EDV, ESV, and SV showed significant difference between the two techniques ($P \leq 0.000$, $P = 0.001$, and $P = 0.000$, respectively). SBH cine imaging with TPAT showed slightly lower EDV, ESV, and SV compared to MBH cine imaging. SBH cine image with TPAT showed a tendency to overestimate myocardial mass in comparison with MBH cine imaging. EF and myocardial mass were not significant different between the two techniques ($P = 0.942$ and $P = 0.625$, respectively). EF and myocardial mass of SBH cine

imaging with TPAT showed good correlation with values of MBH cine imaging in Passing-Bablok regression charts and Bland-Altman plots (Figs. 1, 2). All variables of LV global function and myocardial mass were strongly correlated with each other between the two observers (MBH cine ICC = 0.96-1.0 vs. SBH cine ICC = 0.92-1.0).

Analysis of regional wall motion abnormality was performed for all 50 patients in a total of 1600 segments. Results are shown in Figure 3. In evaluation of regional wall motion abnormality, 493 segments were normal, 153 segments showed hypokinesia, and 154 segments showed akinesia when MBH cine imaging was evaluated. There were 498 segments with normal, 178 segments with hypokinesia, and 124 segments with akinesia when SBH cine imaging was evaluated. Regional wall motion abnormalities were not significantly different between the two acquisition techniques (P = 0.552). Inter-observer agreement between the two observers was excellent (MBH cine k = 0.813 vs. SBH cine k = 0.844).

SNR and CNR were not significantly different between the two techniques. The SNR of SBH cine imaging with TPAT tended to be higher than that of MBH cine imaging (114.1 ± 79.1 vs. 88.6 ± 34.7, P = 0.066). However, the CNR was lower in SBH cine imaging with TPAT compared to that in MBH cine imaging (322.4 ± 243.6 vs. 347.1 ± 157.7, P = 0.377). Values had excellent correlation between the two

Table 1. Global LV Functional Parameters and Myocardial Mass Measured by SBH Cine Imaging with TPAT and MBH Cine Imaging

	SBH cine imaging	MBH cine imaging	P-value
	Mean ± SD	Mean ± SD	
EDV*	195.6 ± 120.0	207.8 ± 125.8	< 0.000
ESV	115.3 ± 107.4	119.7 ± 108.7	0.001
SV*	78.9 ± 31.6	85.6 ± 35.1	0.000
EF	48.9 ± 18.4	48.8 ± 17.8	0.942
MM	152.8 ± 56.9	151.8 ± 56.6	0.625

Global LV function parameters and MM were compared between the two techniques using paired t-test or Wilcoxon signed rank test.

*Data were analyzed using Wilcoxon signed rank test.

EDV = end-diastolic volume; EF = ejection fraction; ESV = end-systolic volume; LV = left ventricular; MBH = multiple breath-hold; MM = myocardial mass; SBH = single breath-hold; SD = standard deviation; SV = Stroke volume.

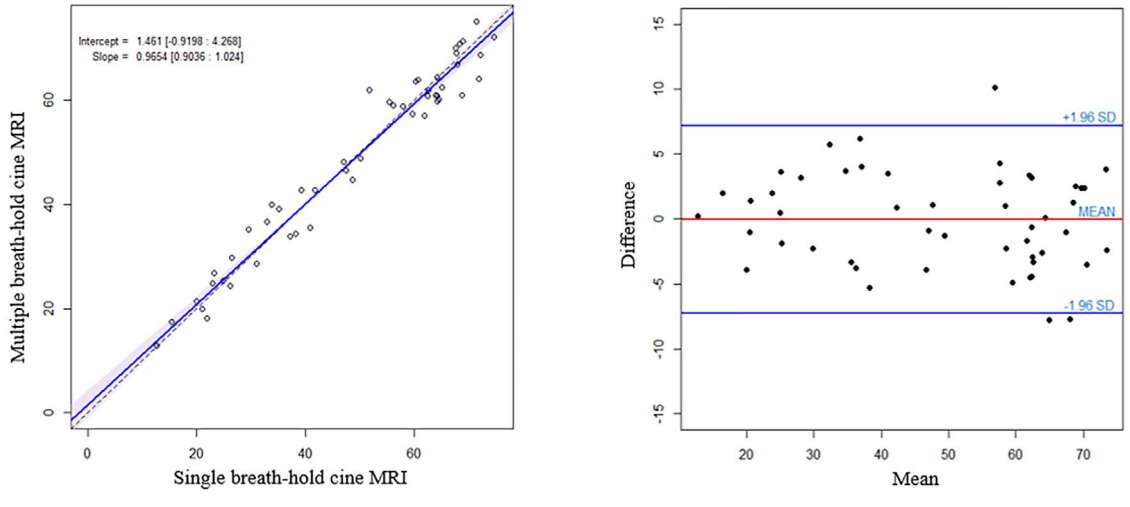

a b

Fig. 1. Passing-Bablok regression chart (a) and Bland-Altman plot (b) of EF obtained from SBH and MBH hold cine imaging. EF values in SBH cine imaging with TPAT showed good correlation with those in MBH cine imaging. EF = ejection fraction; MBH = multiple breath-hold; SBH = single breath-hold; TPAT = temporal parallel acquisition technique

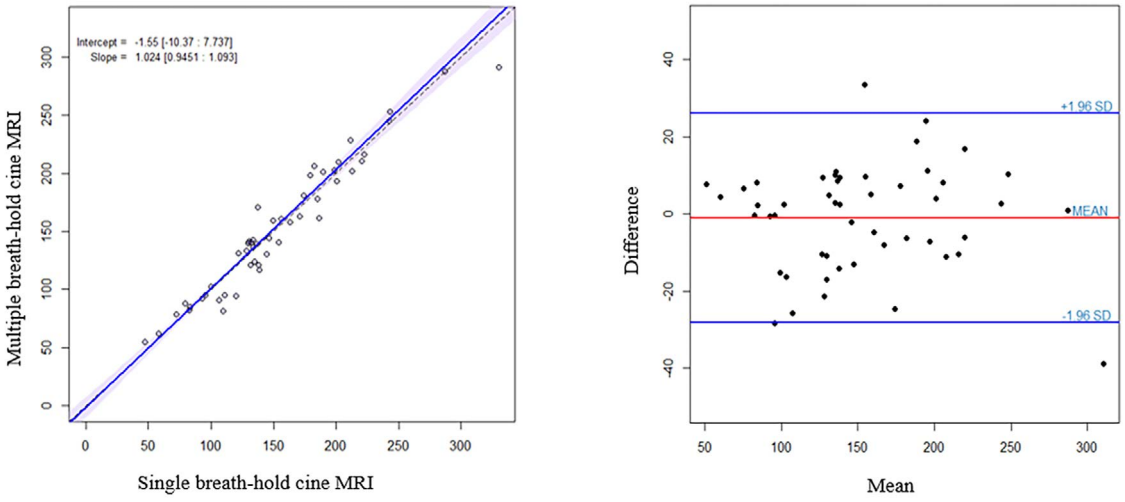

a b

Fig. 2. Passing-Bablok regression chart (a) and Bland-Altman plot (b) of myocardial mass obtained from SBH and MBH cine imaging. Myocardial mass in SBH cine imaging with TPAT was correlated with that in MBH cine imaging. SBH cine imaging with TPAT revealed a tendency to overestimate myocardial mass compared to MBH cine imaging. MBH = multiple breath-hold; SBH = single breath-hold; TPAT = temporal parallel acquisition technique

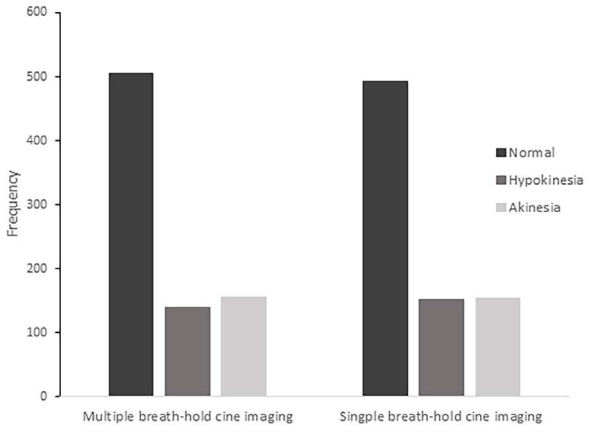

Fig. 3. Distribution of regional wall motion abnormality evaluated by two acquisition techniques (n = 800 segments in each technique). Regional wall motion abnormality was not significantly different between the two acquisition techniques (P = 0.552).

observers (ICC, 0.85; 95% confidence interval, 0.80-0.89).

DISCUSSION

TPAT-accelerated SBH cine imaging results were correlated with MBH cine imaging results. No significant difference in the assessment of LVEF or LV myocardial mass was found between the two techniques. In regional wall motion abnormality analysis, the two acquisition techniques showed no significant difference either. SNR and CNR of SBH cine imaging with TPAT were not significantly different compared with those of MBH cine imaging. However, CNR in SBH cine imaging tended to be lower than that in MBH cine imaging. Previous studies have demonstrated that global LV function and regional wall motion have adequate agreement between MBH and SBH cine imaging in healthy people and patients with acute myocardial infarction (7, 14-16). However, the accuracy of SBH cine imaging with TPAT for evaluating global and regional LV function in patients with arrhythmia has not been described. Our study demonstrated the feasibility of SBH cine imaging with TPAT for the evaluation of global and regional LV function in patients with cardiac arrhythmia.

MBH cine imaging with an SSFP sequence has been widely considered the gold standard for assessing LV function due to its excellent accuracy and reproducibility (11). However, this technique compromises image quality. In addition, assessment of LV function is limited in ECG-synchronized cine acquisition with SSFP for patients with arrhythmia (Fig. 4) (17, 18). MBH cine imaging may also fail in patients who cannot tolerate repeated breath-holds. Acceleration techniques that can acquire multiple

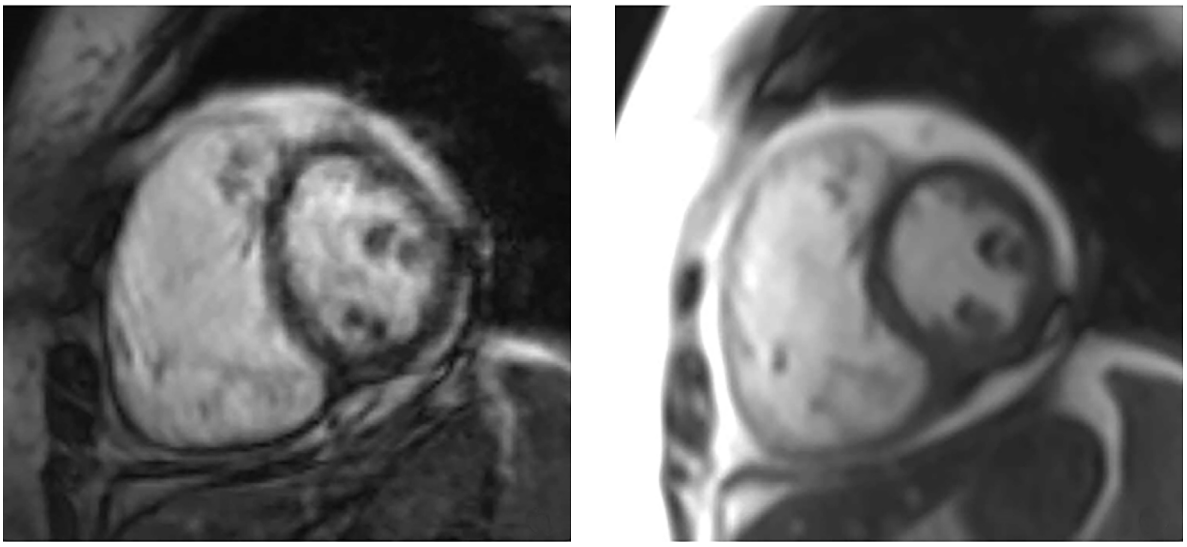

a b

Fig. 4. Mid-ventricular short-axis images of a 78-year-old female with atrial fibrillation obtained with MBH cine imaging (a) or SBH cine imaging with TPAT (b). MBH cine imaging resulted in blurring of the myocardium.

cine images with SBH are gradually becoming available for routine clinical use (14). TPAT has been used for functional analysis in terms of scan time, image quality, and spatial or temporal resolution (7, 19). Additionally, SBH multi-slice imaging using TPAT may reduce slice misalignment effects of cardiac motion due to respiration (7, 20). In previous studies, several strategies have been examined to determine LV function with TPAT (14, 21-24). Accelerated SBH imaging in combination with a guide-point modeling post-processing technique might be useful for rapid evaluation of accurate LV function. However, accurate evaluation of LV function using regional wall motion abnormality is compromised by limited section of LV myocardium (7, 24). Therefore, whole myocardial coverage and rapid image acquisition are required for clinical evaluation.

In previous studies, EDV and ESV for SBH cine imaging with TPAT tend to be relatively low (5, 7, 16). Wintersperger et al. (5) have reported that CNR is decreased with increased acceleration (51% decrease at acceleration factor [R] = 4, 86% decrease at R = 7) and that CNR losses are accompanied by a reduction in image quality. Hunold et al. (25) have revealed a 34-49% reduction in SNR for R = 2. SNR and CNR loss can impair the visualization of small endocardial trabeculation, resulting in inferior delineation of endocardial trabeculation which may have led to underestimation of LV volumetric parameters (7, 16). Results of our study were consistent with these findings. Values of EDV and ESV in SBH cine imaging with TPAT tended to be smaller than those measured in MBH cine imaging. In our study, underestimation of EDV, ESV, and SV on SBH cine image might be due to low frame number (image number/RR interval) (30 in MBH technique vs. 10.3 ± 2.8 in SBH technique). However, the SBH cine imaging with TPAT overestimated the LV mass (152.8 ± 56.9 vs. 151.8 ± 56.6). Wintersperger et al. (16) have demonstrated that accelerated cine MR imaging can overestimate the average myocardial segment thickness due to SNR and CNR loss. Overestimation of wall thickness for lower tendency of CNR in TPAT might have contributed to the overestimation of LV mass in our study.

Several studies have analyzed regional wall motion using SBH TPAT imaging. Nassenstein et al. (7) have shown that regional wall motion is not significantly different between single-slice imaging and SBH multi-slice imaging. In our study, MBH cine imaging encompassed 30 images while SBH cine imaging encompassed 6 to 12 images. In spite of the small number of acquired images, analysis of regional wall motion abnormalities of SBH cine imaging using TPAT was not significantly different compared to that with MBH cine imaging.

This study has several limitations. First, this was a retrospective study. Various types of arrhythmia were included. Second, image acquisition at various acceleration factors was not performed. In addition, we could not suggest a strategy that might produce optimal image quality in patients with arrhythmia. The final limitation to

this study was its small sample size. Subsequent studies with larger populations of patients with arrhythmia are needed to validate our results.

Our study demonstrated that SBH cine imaging with TPAT could permit rapid acquisition with results comparable to those of conventional MBH cine imaging for global and regional LV function in patients with arrhythmia. Therefore, SBH cine imaging with TPAT instead of MBH cine imaging may be useful for patients with arrhythmia to assess LV function in light of patient comfort.

Acknowledgments

This work was supported by Korean study group of Cardiovascular Magnetic Resonance (KCMR) in Korean Society of Magnetic Resonance in Medicine (KSMRM).

Declaration of Conflict of interest

The authors have no conflicts of interest to declare.

REFERENCES

1. Rokey R, Wendt RE, Johnston DL. Monitoring of acutely ill patients during nuclear magnetic resonance imaging: use of a time-varying filter electrocardiographic gating device to reduce gradient artifacts. Magn Reson Med 1988;6:240-245
2. Juergens KU, Fischbach R. Left ventricular function studied with MDCT. Eur Radiol 2006;16:342-357
3. Bak SH, Ko SM, Jeon HJ, Yang HS, Hwang HK, Song MG. Assessment of global left ventricular function with dual-source computed tomography in patients with valvular heart disease. Acta Radiol 2012;53:270-277
4. Niendorf T, Sodickson DK. Highly accelerated cardiovascular MR imaging using many channel technology: concepts and clinical applications. Eur Radiol 2008;18:87-102
5. Wintersperger BJ, Reeder SB, Nikolaou K, et al. Cardiac CINE MR imaging with a 32-channel cardiac coil and parallel imaging: impact of acceleration factors on image quality and volumetric accuracy. J Magn Reson Imaging 2006;23:222-227
6. Cawley PJ, Maki JH, Otto CM. Cardiovascular magnetic resonance imaging for valvular heart disease: technique and validation. Circulation 2009;119:468-478
7. Nassenstein K, Eberle H, Maderwald S, et al. Single breath-hold magnetic resonance cine imaging for fast assessment of global and regional left ventricular function in clinical routine. Eur Radiol 2010;20:2341-2347
8. Vincenti G, Monney P, Chaptinel J, et al. Compressed sensing single-breath-hold CMR for fast quantification of LV function, volumes, and mass. JACC Cardiovasc Imaging 2014;7:882-892
9. Saremi F, Grizzard JD, Kim RJ. Optimizing cardiac MR imaging: practical remedies for artifacts. Radiographics 2008;28:1161-1187
10. Pruessmann KP, Weiger M, Scheidegger MB, Boesiger P. SENSE: sensitivity encoding for fast MRI. Magn Reson Med 1999;42:952-962
11. Bassett EC, Kholmovski EG, Wilson BD, et al. Evaluation of highly accelerated real-time cardiac cine MRI in tachycardia. NMR Biomed 2014;27:175-182
12. Cerqueira MD, Weissman NJ, Dilsizian V, et al. Standardized myocardial segmentation and nomenclature for tomographic imaging of the heart. A statement for healthcare professionals from the Cardiac Imaging Committee of the Council on Clinical Cardiology of the American Heart Association. Circulation 2002;105:539-542
13. Nucifora G, Muser D, Masci PG, et al. Prevalence and prognostic value of concealed structural abnormalities in patients with apparently idiopathic ventricular arrhythmias of left versus right ventricular origin: a magnetic resonance imaging study. Circ Arrhythm Electrophysiol 2014;7:456-462
14. Kozerke S, Plein S. Accelerated CMR using zonal, parallel and prior knowledge driven imaging methods. J Cardiovasc Magn Reson 2008;10:29
15. Theisen D, Sandner TA, Bamberg F, et al. High-resolution cine MRI with TGRAPPA for fast assessment of left ventricular function at 3 Tesla. Eur J Radiol 2013;82:e219-224
16. Wintersperger BJ, Sincleair S, Runge VM, et al. Dual breath-hold magnetic resonance cine evaluation of global and regional cardiac function. Eur Radiol 2007;17:73-80
17. Duarte R, Fernandez-Perez G, Bettencourt N, et al. Assessment of left ventricular diastolic function with cardiovascular MRI: what radiologists should know. Diagn Interv Radiol 2012;18:446-453
18. Feng L, Srichai MB, Lim RP, et al. Highly accelerated real-time cardiac cine MRI using k-t SPARSE-SENSE. Magn Reson Med 2013;70:64-74
19. Niendorf T, Sodickson DK. Parallel imaging in cardiovascular MRI: methods and applications. NMR Biomed 2006;19:325-341
20. Chandler AG, Pinder RJ, Netsch T, et al. Correction of misaligned slices in multi-slice cardiovascular magnetic resonance using slice-to-volume registration. J Cardiovasc Magn Reson 2008;10:13
21. Breuer FA, Kellman P, Griswold MA, Jakob PM. Dynamic autocalibrated parallel imaging using temporal GRAPPA (TGRAPPA). Magn Reson Med 2005;53:981-985

22. Nael K, Ruehm SG, Michaely HJ, et al. High spatial-resolution CE-MRA of the carotid circulation with parallel imaging: comparison of image quality between 2 different acceleration factors at 3.0 Tesla. Invest Radiol 2006;41:391-399
23. Heilmaier C, Nassenstein K, Nielles-Vallespin S, Zuehlsdorff S, Hunold P, Barkhausen J. Assessment of left ventricular function with single breath-hold highly accelerated cine MRI combined with guide-point modeling. Eur J Radiol 2010;74:492-499
24. Eberle HC, Nassenstein K, Jensen CJ, et al. Rapid MR assessment of left ventricular systolic function after acute myocardial infarction using single breath-hold cine imaging with the temporal parallel acquisition technique (TPAT) and 4D guide-point modelling analysis of left ventricular function. Eur Radiol 2010;20:73-80
25. Hunold P, Maderwald S, Ladd ME, Jellus V, Barkhausen J. Parallel acquisition techniques in cardiac cine magnetic resonance imaging using TrueFISP sequences: comparison of image quality and artifacts. J Magn Reson Imaging 2004;20:506-511